

Adhesion and clustering of charge isomers of myelin basic protein at model myelin membranes[☆]

L.V. Shanshiashvili,^{a,b} N.Ch. Suknidze,^a G.G. Machaidze,^{a,b} D.G. Mikeladze,^a
and J.J. Ramsden^{b,c,*}

^a *I.S. Beritashvili Institute of Physiology, Georgian Academy of Sciences, Tbilisi, Georgia*

^b *Department of Biophysical Chemistry, Biozentrum of the University, Basel, Switzerland*

^c *Collegium Basilea (Institute of Advanced Study), Hochstrasse 51, 4053 Basel, Switzerland*

Received 7 May 2003, and in revised form 4 September 2003

Abstract

The association of myelin basic protein charge isomers with the lipid part of the myelin membrane was investigated at the microscopic (molecular) level in a model membrane system, using optical waveguide lightmode spectrometry to determine with high precision the kinetics of association and dissociation to planar phospholipid membranes under controlled hydrodynamic conditions and over a range of protein concentrations. Detailed analysis of the data revealed a rich and intricate behaviour and clearly showed that the membrane protein affinity is characterized by at least four independent parameters: (i) the association rate coefficient characterizing the protein–membrane interaction energy as the protein approaches the fluid–membrane interface; (ii) the protein–membrane adhesion, i.e., the probability that it will remain at the membrane after arrival; (iii) the protein conformation at the membrane; and (iv) the protein's tendency to cluster at the membrane. Some of these parameters varied in characteristic ways as the bulk solution concentration of the protein was varied, giving further clues to the detailed molecular compartment of the protein. The parameters and their characteristic variations with bulk concentration were markedly different for the different isomers. Implications of these results for neurological disorders involving demyelination, such as multiple sclerosis, are discussed.

© 2003 Elsevier Inc. All rights reserved.

Keywords: Adsorption; Association; Desorption; Multiple sclerosis; OWLS

Myelin basic protein (MBP)¹ is a major component of the myelin sheath surrounding the axons of the central nervous system (CNS), constituting about a fifth of the total myelin protein, which makes up about a third of the dry weight of the sheath material, the rest being lipids [1]. MBP is a water-soluble membrane protein, which interacts with apposed cytoplasmic surfaces of the myelin membrane and plays an important role in the formation and maintenance of myelin [2,3]. The integ-

rity of the myelin sheath to a large extent depends on the interactions of MBP with the other myelin proteins and the different lipids in the bilayer, and with cytoskeleton proteins such as actin and tubulin in oligodendrocytes, and in compact myelin in which actin and tubulin occur in the radial component, i.e., a series of tight junctions passing through many layers of myelin [4–7]. Intensified breakdown of myelin membranes takes place in neurological disorders such as multiple sclerosis (MS), the severity of the symptoms depending on the degree of axon demyelination. The degradation of the myelin sheath is induced by an autoimmune response involving T-cell attack of MBP [8].

It has been established that MBP occurs in vivo in several isoforms of different molecular weights (14,000, 17,000, 18,500, and 21,500), generated by alternative splicing of the gene (see, e.g. [9]). These isoforms in turn have several charge isomers produced by

[☆] Supported by INTAS Grant No. 97-1561.

* Corresponding author. Fax: +41-61-361-95-23.

E-mail address: J.Ramsden@unibas.ch (J.J. Ramsden).

¹ *Abbreviations used:* CNS, central nervous system; HPLC, high pressure liquid chromatography; MS, multiple sclerosis; MBP, myelin basic protein; OWLS, optical waveguide lightmode spectrometry; PAGE, polyacrylamide gel electrophoresis; PC, 1-palmitoyl-2-oleoyl-sn-glycero-3-phosphatidylcholine; PS, phosphatidylserine; r.i.i., refractive index increment.

posttranslational modifications (serine and threonine phosphorylation, arginine deimination, and glutamine deamidation) of specific amino acids [10,11]. These isomers are expected to have different affinities for the myelin membrane, which provides a possible clue to the cause of demyelination, which would be enhanced by the transformation of MBP into less adhesive forms. A present difficulty in testing this hypothesis is that ‘adhesion’ of the protein has not been well defined in the literature. Our first aim in this paper was to overcome this difficulty by providing a physico-chemical framework (model) for discussing protein adhesion. Our second aim was to measure the parameters of the model at an appropriate level of accuracy. Our third aim was to compare these parameters for the charge isomers of the 18.5 kDa isoform and correlate the results with the pathology of multiple sclerosis.

The 18.5 kDa isoform is the major one in humans and exhibits charge microheterogeneity as a result of post-translational modification such as loss of C-terminal arginine, deamidation, phosphorylation, and oxidation of methionine to methionine sulfoxide [12,13]. Certain patterns of microheterogeneity are correlated with the incidence of MS and possibly other neurodegenerative diseases [9]. Zand et al. [11] suggested that the post-translational modifications direct specific placement in the myelin membrane, but did not suggest by what mechanism the specific placement might take place. It has been shown that the modification of arginine to citrulline affects antigen recognition and may thus be a factor in the autoimmune response involved in the pathogenesis of MS [14]: an MBP isomer isolated from a patient who died with acute fulminating MS was found to have 18 of the 19 arginines deiminated to citrulline [15].

Hitherto, MBP affinities have only been characterized indirectly by the ability of the protein to aggregate vesicles containing acidic phospholipids [16]; Wood and Moscarello [10] thereby established that the unmodified, most positively charged C1 isoform is the most effective, and the C8 isoform (in which six arginine residues are converted to citrulline) is the least effective as an aggregating agent, and Boggs et al. [16] established that increasing KCl concentration increased the ability of all isomers to aggregate vesicles. This assay does not seem able to distinguish between vesicle cross-linking due to a protein with two accessible binding sites for lipid membranes, or due to proteins with which the membranes become coated, their conformation becoming altered by association with the lipid membrane, and the altered forms having an enhanced affinity for each other. In any case, for an object as complex as a protein, ‘‘affinity’’ is a subtle concept, requiring careful definition before it can be related to the amino acid composition of the polypeptide chain. ‘‘Affinity’’ cannot usually be reduced to a single parameter, let alone correlated with an indirect one such as ‘‘vesicle aggregating ability’’ [17].

Considering such results as are available, it becomes reasonable to propose that the crucial parameters characterizing the system are the affinities of the isomers for the lipid membranes, and for each other once they are adsorbed at the membrane, and furthermore to propose that these affinities depend on the electrostatic charge of the protein, both directly and via the particular protein conformation, which may be associated with a particular charge state. Moreover, MBP is present at such a high concentration at the membrane that it is plausible to propose that particular arrangements of MBP might be decisive in determining the physiological properties of myelin. Hence, we wish to characterize not only the affinity of an individual protein for the membrane, but also the susceptibility of the protein to cluster at the membrane. Ultimately, we wish to trace the occurrence of neurodegenerative diseases to their possible molecular origins.

Our approach to characterizing the protein–lipid interaction is to monitor the kinetics of MBP association and dissociation to and from model planar lipid bilayers under controlled hydrodynamic conditions (see [17] for the general background to this approach). The lipid membrane is supported on a hydrated smooth planar optical waveguide, and the spectrum of guided modes is measured and used to determine the actual number of MBP molecules bound to the membrane at any instant of time [18]. The planar geometry seems to be a better approximation to the low curvature of the myelin sheath (diameter typically up to 15 μm) than the small, highly curved vesicles previously used for affinity studies. Moreover, the planar geometry makes it easy to analyse the data with true heterogeneous kinetics, rather than the ‘pseudohomogeneous’ approximation which was used for the experiments with vesicles. Through careful analysis of the association and dissociation kinetics, it was possible to give a far more detailed and exact characterization of the interaction between MBP and its lipid membrane than has been achievable hitherto, and hence to make a significant step towards the ultimate goal of linking the molecular parameters of the protein–membrane system with those of neurodegenerative diseases.

Experimental procedures

Protein isolation, purification, and characterization

MBP was isolated from bovine brain white matter according to the method of Chou et al. [12] with minor modifications. The acid soluble material was dissolved in 0.08 M glycine buffer (pH 9.6) containing 6 M urea and applied to a CM 52 cellulose cation exchange column equilibrated in the same glycine–urea buffer, except that the pH was 10.5. Following application of the

sample, passage of the pH 10.5 buffer continued until the first peak was completely eluted. The remaining components were eluted from the column using a linear NaCl gradient (0–0.3 M). Afterwards they were dialysed overnight against water at 4 °C. Further purification of the isoforms was carried out by HPLC on a C₁₈ Nova-Pak column (Waters) using a trifluoroacetic acid (0.05%)–acetonitrile (0–60%) gradient. PAGE was used to verify the purity of the isomers. The purified proteins were lyophilized and stored until use at –20 °C. Table 1 lists the amino acid modifications of the isomers.

The refractive index increment (r.i.i.) required for the determination of the number of lipid-bound protein molecules was determined for the C8 isomer in standard buffer (see Solutions) using an LI-3 Rayleigh interferometer (Carl Zeiss, Jena, Germany) as 0.361 cm³/g.

Membrane preparation

Synthetic 1-palmitoyl-2-oleoyl-*sn*-glycero-3-phosphatidyl choline (PC) and phosphatidylserine (PS) were supplied by Avanti (Alabaster, Alabama). A 0.922:0.078 PC:PS mixture (mole fractions) corresponding to the composition used by Wood and Moscarello [10] was spread on a laboratory-built Langmuir trough with which lipid bilayers were assembled on smooth planar optical waveguides as described by Ramsden [19]. The waveguides had the composition Si_{0.62}Ti_{0.38}O₂ and a surface roughness (determined using atomic force microscopy) of 0.09 nm, and were obtained from Artificial Sensing Instruments AG, Zürich, Switzerland (type 2400); they have a thin waveguiding layer optimized for detecting changes in the transverse electric (TE) and transverse magnetic (TM) guided modes with the highest

possible sensitivity [20]. A layer of water ca. 2–3 nm thick (cf. [21]) between the waveguide and the lipid ensures that the membrane has a fluidity comparable to that of the physiological state.

Optical waveguide lightmode spectrometry

The membrane-coated waveguides were assembled into a flow-through cuvette (see, e.g. [22]) and mounted in the measuring head of an IOS-1 integrated optics scanner (Artificial Sensing Instruments) [23]. The effective refractive indices of the zeroth order TE and TM modes were continuously monitored during the following three consecutive stages: (i) buffer flow; (ii) MBP solution flow (over a range of bulk protein concentrations c_b from 2 to 100 µg/cm³); and (iii) buffer flow. Flow was always laminar at a wall shear rate of 22.4 s⁻¹ and controlled by a precision syringe pusher (B. Braun Melsungen AG). The temperature was maintained at 25.0 ± 0.2 °C. The effective refractive indices were converted into numbers (ν) of adsorbed MBP molecules (or total adsorbed protein mass $M = m\nu$, where m is the mass of one molecule of MBP) per unit area of membrane (see e.g., [24] for the full set of equations).

Solutions

The standard buffer used throughout was 10 mM *N*-2-hydroxyethylpiperazine-*N'*-2-ethanesulphonic acid (Hepes)–NaOH, (pH 7.2) with the addition of 0.1 M NaCl (Merck analytical grade) and 1 mM ethylenediaminetetraacetic acid (EDTA). Water purified by a “Nanopure” installation (Barnstead, Dubuque, Ohio) was used throughout. Protein solutions were prepared at concentrations c_b of 2, 5, 10, 20, 50, and 100 µg/ml.

Results

Fig. 1A shows two representative adsorption/desorption curves. For all isoforms, the amount adsorbed gradually approached a plateau, i.e., dM/dt approaching zero, indicative of the jamming of the surface by the binding of at most a protein monolayer to the membrane. Comparing the different isoforms qualitatively, C1, the most cationic isomer of MBP (see Table 1), was the most effectively² adsorbed on the lipid membrane, C2 was less effective than C1, and C8 less effective than C2. The phosphorylated isoforms C3 and C4 were less effective than C8 and the least effective was C7. As the bulk concentration of protein was increased, the

Table 1
Characteristics of the charge isomers of the 18.5 kDa charge isoform of MBP (from [11])

Designation	n_{phos}^a	n_{deim}^b	n_{deamid}^c	Rel. charge
C1	0	0	0	0
C2	0	0	1	–1
C3	1S+1T	0	0	–2
C4	2S+1T	0	0	–3
C5	3S+1T	0	0	–4
C6	4S+1T	0	0	–5
C7	≥4S+≥1T	>5	0	–
C8 ^d	0	5	0	–6

^a Estimated numbers of phosphorylated serines (S) and threonines (T).

^b Estimated numbers of deiminated arginines (i.e., converted to citrulline).

^c Estimated numbers of deamidated glutamines (i.e., converted to glutamic acid).

^d This form (which has an isoelectric point of 10.3) is usually denoted “least charged” because it elutes first on the cationic column. The isoelectric point of the mixture of isoforms is 10.5.

^e unknown; no data available.

² ‘Effectively’ is used here purely for the sake of comparison with the earlier vesicle aggregation work [10,16], and merely has the loose meaning that the more effective an isomer, the more it is adsorbed at the membrane.

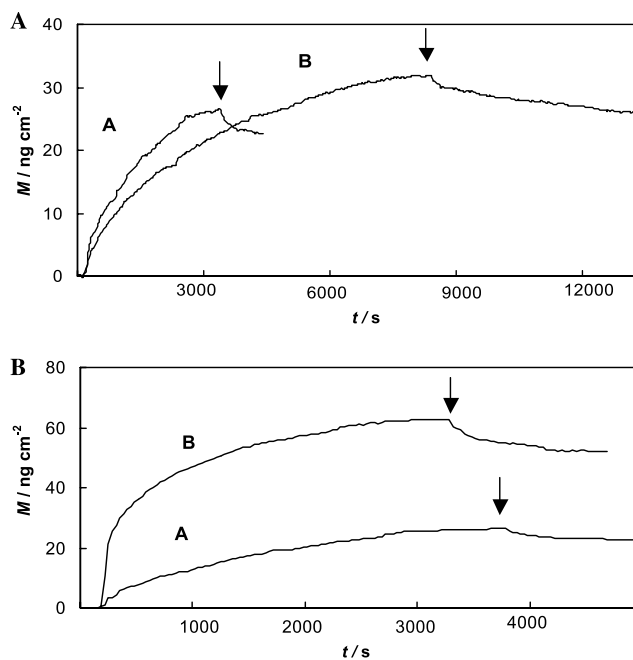


Fig. 1. Typical adsorption/desorption kinetics (plots of adsorbed amount of protein versus time). C1 (A) and C8 (B), both at a bulk concentration $c_b = 20 \mu\text{g/ml}$. (B) C8 at bulk concentrations of 20 (A) and $100 \mu\text{g/ml}$ (B). The arrows mark when the bulk concentration c_b was set to zero.

amounts at jamming (“saturation”) also increased, although much less linearly than with concentration (see an example in Fig. 1B). Desorption was strongly non-exponential: in most cases, after a small proportion of protein was removed rapidly upon initiating protein-free buffer flow, removal slowed down dramatically.

Quantitative evaluation

The data are described by the general equation for association–dissociation kinetics at the solid–liquid interface (see e.g., [17]):

$$dv/dt = k_a c_v \phi(v) - k_d(t)v, \quad (1)$$

where k_a and k_d are, respectively, the association and dissociation rate coefficients, c_v is the dissolved protein concentration in the vicinity of the membrane surface, and ϕ is the available area function which gives the fraction of the total membrane surface which is available to accept a protein from solution.

c_v can be calculated from c_b by writing the differential equation for the former (assuming convective–diffusive conditions):

$$V \frac{dc_v}{dt} = S \left[\frac{D^{2/3} (h\gamma)^{1/2} (c_b - c_v)}{3\kappa^{1/6} (6s)^{1/2}} + k_d(t)v - k_a c_v \phi(v) \right], \quad (2)$$

where V and S are unit volume and surface, respectively, D is the protein diffusivity ($5.4 \times 10^{-7} \text{ cm}^2/\text{s}$), h is the

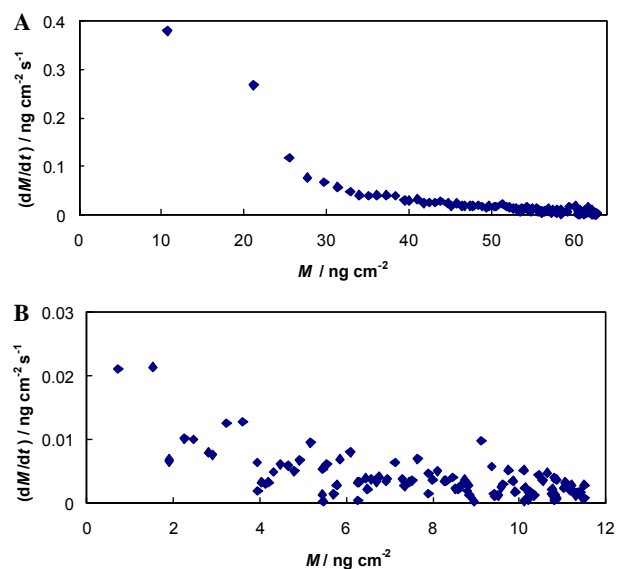


Fig. 2. Adsorption data from Fig. 1 replotted as rate of the adsorption versus the amount adsorbed. (A) C8, $c_b = 100 \mu\text{g/ml}$. (B) C1, $c_b = 20 \mu\text{g/ml}$.

cuvette height (0.314 mm), κ is the kinematic viscosity (the value for pure water, $9 \times 10^{-3} \text{ cm}^2/\text{s}$, was taken), and s is the distance from the flow inlet to the center of the measuring zone (3.5 mm). Allowing the left-hand side to go to zero yields an expression solvable for c_v (see [17] for a more comprehensive discussion of this procedure).

By plotting the rate of association dv/dt against v (see a representative example in Fig. 2), it was ascertained that the association kinetics was in all cases consistent with generalized ballistic deposition (GBD) [25].³ This process comprises three possible fates for a protein arriving at the membrane: (i) adsorption at the exact spot at which it first arrives at the membrane; (ii) adsorption next to a previously adsorbed protein; and (iii) departure of the protein back into solution. If the protein arrives centered on a spot around which there is sufficient space for it to adsorb, it does so with probability p' (process i), or otherwise it departs (process iii); if it arrives at a spot that does not permit it to adsorb (since adsorption would cause the molecule to overlap a previously adsorbed one), it moves laterally until it comes to a spot that does allow enough area to adsorb (which will be immediately adjacent to a previously adsorbed protein), upon which it does so with probability p (process ii), otherwise departs (process iii). The lateral movement takes place via correlated lateral diffusion in the immediate vicinity of the interface [26].

³ The expression ‘ballistic’ comes from the fact that the ballistic deposition (BD) model was first developed to describe relatively large particles settling on a surface under the influence of gravity, which plays no role in our case.

Adsorption via GBD is characterized by three parameters (cf. Eq. (1)): k_a , which scales the overall rate; the area a occupied at the membrane by the protein, which fixes the overall probability of finding space to adsorb via either process (i) or process (ii); and j , the ratio of probabilities p/p' ; $j = 0$, the lowest possible value, corresponds to pure random sequential association ($p = 0$) [27], and higher values correspond to a tendency of the proteins to form two-dimensional clusters at the surface, with the limit of $p' = 0$ corresponding to reaction-limited aggregation. Hence, j can be considered as a quantitative measure of the homophilicity of the membrane-associated protein (j increasing with increasing homophilicity).

The parameters a , j , and k_a were obtained by fitting the numerically differentiated adsorption data to Eq. (1), replacing ϕ by the GBD expression appropriate for spheres [28]

$$\phi = 1 + f_1(j)\theta + f_2(j)\theta^2 + f_3(j)\theta^3, \quad (3)$$

where θ is the fractional surface coverage, related to v by

$$\theta = va, \quad (4)$$

and with

$$f_1 = 4(j - 1), \quad (5)$$

$$f_2 = 3.808 - 0.180j - 3.128j^2 \quad (6)$$

and

$$f_3 = 1.407 + 4.679j - 25.58j^2 + 8.550j^3. \quad (7)$$

The maximum observed value of v (denoted v_{\max}) was recorded. By virtue of Eq. (4), it should correspond to the jamming limit θ_J (since θ_J is approached asymptotically, v_{\max} gives a lower limit for θ_J). Using the value of $\theta_J = 0.55$ for spheres [29], we found good agreement between a determined by fitting the kinetics as described above, and a estimated from $a \approx \theta_J/v_{\max}$ (from Eq. (4)).

Since complete desorption would have required tens or hundreds of hours, we characterized it by fitting the empirical function

$$v(t) = (v_0 - v_\infty)e^{-k_d t} + v_\infty \quad (8)$$

to the measured portion (the flux of protein-free solution was continued until $v(t)$ appeared practically constant on a linear timescale), where v_0 is the value immediately before starting desorption (at $t = 0$) and v_∞ the “irreversible” residue, with v_∞ and k_d as the fitting parameters. We then calculated the parameter

$$\mathcal{D} = 1 - v_\infty/v_0 \quad (9)$$

as a measure of desorbability. The parameters k_a , a , j , and \mathcal{D} are collected in Table 2.

Discussion

Many of the characteristic parameters gathered in Table 2 were found to vary monotonically with bulk protein concentration c_b . Below we consider this behaviour and its implications for each of the four fitted parameters in turn. The differences between the different isomers are summarized in Table 3.

a, area per molecule, an indication of protein conformation and packing

All the individual proteins show a decrease in a with increasing c_b . This clearly indicates conformational change at the surface [17,30,31]: the (relatively slow) change is blocked by the rapid arrival of adsorbed neighbours. Electron microscopy together with molecular models of MBP (C1) adsorbed to a lipid monolayer in 10 mM Hepes + 150 mM NaCl + 10 mM CaCl₂ [32,33] has revealed a roughly globular protein opened out somewhat to form a C-shaped molecule with inner and outer radii of 3 and 5.5 nm, respectively, and a thickness of 4.7 nm (Fig. 3). Hence, it should occupy 80–100 nm² upon adsorption, compared with 15–30 nm² for a compact protein sphere of the same molecular weight. Our results (Table 2) indicate a considerable range of conformational changes at the membrane, ranging from presumed extreme denaturation (areas between 215 and 245 nm²) for C4 and C7 adsorbed from the most dilute solutions, to extreme, presumably membrane-induced, compactification for adsorption from the most concentrated solutions (especially in the case of C8).

Table 2
Association and dissociation parameters, for the bulk concentration range 2–100 µg/ml

Designation	a (nm ²)	k_a (cm s ⁻¹ × 10 ⁻⁵)	j	\mathcal{D}
C1	25–13	30–0.06	0.05 ± 0.04	0.08 ± 0.08
C2	31–13	14–0.30	0.05 ± 0.04	0.08 ± 0.04
C3	110–30	1.3–0.07	0.2–0.03	0.94–0.10
C4	215–18	0.22–0.12	0.6–0.04	0.49–0.13
C7	245–14	0.14–0.11	0.5–0	0.90–0.16
C8	83–9	0.7 ± 0.3	0.04–0	0.05–0.38

Uncertainties in the individual values are about ±20%. See Eqs. (4), (1), and (9), respectively, for the definitions of a , k_a and \mathcal{D} ; $j = p/p'$ (see ‘Results’ and Eq. (3)).

Table 3

The order of variation among the measured kinetic parameters a , k_a , and \mathcal{D} , compared with the order of electrostatic charge and phosphorylation of the isomers

Parameter	c_b	Order
From Table 1		
Charge ^a	–	C8 > C6 > C5 > C4 > C3 > C2 > C1
Phosph. ^b	–	C7 > C6 > C5 > C4 > C3 ~ C2 ~ C1 ~ C8
From Table 2		
a	Low	C7 > C4 > C3 > C8 > C2 > C1
	High	C3 > C4 ~ C7 ~ C2 ~ C1 ~ C8 ^c
k_a	Low	C1 > C2 > C3 > C8 > C4 > C7
	High	C8 > C2 > C4 > C7 > C3 ~ C1
\mathcal{D}	Low	C3 ~ C7 > C4 > C1 ~ C2 ~ C8
	High	C8 > C7 > C4 > C3 > C2 ~ C1

^a Starting with the most negative (C7 has not yet been characterized).

^b Degree of phosphorylation.

^c Differences much less marked than at low c_b .

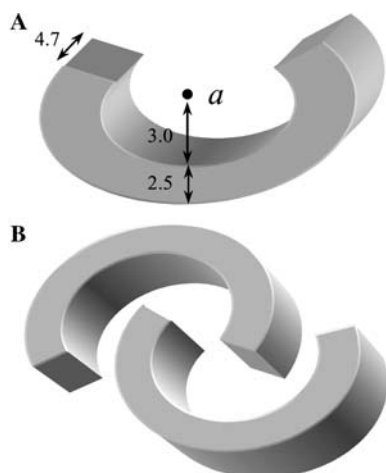


Fig. 3. (A) Sketch of the molecular shape and size (all dimensions in nm) of myelin basic protein (MBP), inferred from [32]. (B) Sketch of how two molecules might interpenetrate, thus reducing their areas at the surface.

j , the homophilicity or clustering parameter

Except for C1 and C2, j decreased with increasing c_b . C3, C4, and C7 showed a substantial degree of clustering at low bulk solution concentrations, but tended to pure random sequential adsorption (RSA) at high concentrations, and C1, C2, and C8 are close to RSA at all concentrations. This is typical evidence for ordered or semi-ordered two-dimensional arrays being the origin of the large areas per molecule (cf. [34]), which actually then correspond to the unit cell size. The areas seem too large for a denatured protein, and since they only are seen at the lowest bulk concentrations, which would favour dissociation of solution oligomers, it is unlikely that they correspond to the adsorption of oligomers. Note too that the large areas were observed for the

heavily phosphorylated forms C4 and C7, which are believed to be the most stable (cf. the discussion on p. 4262 in [32]), and hence the least likely to denature. Phosphorylation appears to promote clustering, with these most heavily phosphorylated forms giving the highest j values.

k_a , derived from the adsorption energy barrier

The higher the long-range protein–membrane repulsion (i.e., the energy barrier the molecule has to surmount prior to adsorption; the initial measured rate of adsorption was always less than the diffusion limited rate), the smaller is k_a [17,35]. The observed differences between the different isomers correspond, at low c_b , almost precisely to the order of decreasing positive charge. Hence, we can infer that the adsorption energy barrier is dominated by electrostatic forces and that phosphorylation exerts a definite inhibitory effect over and above that due to the augmentation of electrostatic repulsion. The different order at high c_b (and, indeed, the fact that k_a is not invariant with c_b) hints at a different kind of adsorption mechanism starting to operate, in which the particles interfere with one another before they actually arrive at the surface.

\mathcal{D} , the parameter of adhesion strength

The variations among the isomers correspond to the order of positive charge per molecule, which implies that electrostatic forces govern protein adhesion to the acidic lipid membrane. C1 and C2 are almost irreversibly adsorbed. Regarding the variation with bulk concentration, C3, C4, and C7 become less reversibly adsorbed as c_b increases, i.e., clusters are more reversible, and therefore differ qualitatively from the behaviour of C8, which becomes more reversible as c_b increases (cf. human serum albumin adsorbed on titania, [37]), i.e., crowding facilitates desorption.

Conclusions

The interaction of MBP isomers with acidic phospholipid bilayer membranes exhibits rich and complex behaviour when scrutinized with a technique (optical waveguide lightmode spectrometry, OWLS) that permits the kinetics of accumulation of the protein at the molecular level to be directly inferred accurately and precisely. A single parameter, at best depending on some averaged physico-chemical quantity, is clearly inadequate to characterize the affinity; relevant parameters, showing different variations across the charge isomers, are the area per molecule, the adsorption energy barrier, the homophilicity, and the adhesion strength. The values associated with these parameters

vary across the range of bulk (corresponding to estimated cytoplasmic) concentrations prior to membrane adsorption, further increasing the dimensionality of the requisite parameter space.

The starting point of our thinking, that electrostatic charge is the key parameter that simply alters the affinity of the protein for the membrane, accounts for most of the variation in the adsorption energy barrier and adhesion strength, but it is insufficient to interpret the ensemble of our observations. We therefore hypothesize that:

1. Phosphorylation not only affects electrostatic charge, but also affects protein conformational stability, and hence conformation, especially the compactness of individual molecules. It may be pertinent that circular dichroism and other techniques have shown that the degree of secondary structure, primarily the amount of α -helix, but also of β -sheet, increased substantially after phosphorylation of MBP (in the presence of organic solvents, detergent, and lipids) [38]. The thermodynamically stable structure of MBP in aqueous solution appears to be a highly flexible coil [36], but when bound to bilayers of acidic lipids, MBP appears to acquire substantially more ordered secondary structure than in aqueous solution.
2. Electrostatic charge and phosphorylation determine the packing or clustering of the protein at the bilayer.

Relation to disease

MBP is absolutely required for the formation of myelin and the major dense line, and the regulation of its electrostatic charge could alter the compaction and structure of the myelin sheath. The catalytic activities of the endogenous enzymes such as peptidylarginine deiminase (PAD) [39], or various types of protein kinases like MAP-kinase, protein kinase C or tyrosine protein kinases (e.g. [40]), or methyltransferase [41], which all may participate in the conversion of MBP isomers [42–44], are strongly regulated during periods of increased neuronal activity [45], but the regulation is disrupted during some diseases [9,46]; *fyn* tyrosine kinase-deficient mice are unable to form compact myelin [47]. It is to be inferred that during some pathological conditions the normal ratios of charge isomers are disrupted. It may be relevant to mention that Mastronardi et al. [46] showed that in transgenic mice with a different (nonwild type) copy of the myelin proteolipid protein DM20 the microheterogeneity (which arises through posttranslational events) was changed resulting in a higher proportion of the less cationic components, reminiscent of the changes in MBP found in multiple sclerosis.

Our experimental data show that each charge isomer interacts with lipid bilayer differently. Diminished surface charge density, such as occurs upon citrullination of the arginines of MBP, undoubtedly diminish its inter-

action with the lipids in the myelin membrane, rendering the protein more vulnerable to attack (more accessible) by proteolytic enzymes [41]. Beyond that, changes in posttranslational modifications alter the protein, its adhesion and its compaction, and hence the structure of the myelin sheath as a whole. It may be a highly pertinent result that the heavily citrullinated form C8, strongly implicated in MS, is qualitatively different in its membrane interactions from all the others.

Modulated phosphorylation [44] and citrullination [15] have been clearly correlated in demyelinating disease (multiple sclerosis). The formation of an abnormal myelin sheath would appear to be an ineluctable consequence of these modulated modifications. We do not yet have sufficient clinical data to comprehensively link the stages of the disease as it develops with molecular changes, but we can already infer from our data (Tables 2 and 3) that heavy citrullination will tend to produce demyelination.

References

- [1] N.S. Murthy, D.D. Wood, M.A. Moscarello, *Biochim. Biophys. Acta* 769 (1984) 493–498.
- [2] F.X. Omlin, H.D. Webster, C.G. Palkovits, S.R. Cohen, *J. Cell Biol.* 95 (1982) 242–248.
- [3] C. Readhead, N. Takasashi, H.D. Shine, R. Saavedra, R. Sidman, L. Hood, *Ann. N Y Acad. Sci.* 60 (1990) 280–285.
- [4] G.W. Brady, N.S. Murthy, D.B. Fein, D.D. Wood, M.A. Moscarello, *Biophys. J.* 34 (1981) 345–350.
- [5] P.M. Pereyra, E. Horvath, P.E. Braun, *Neurochem. Res.* 13 (1988) 583–595.
- [6] J. Karthigasan, B. Kosaras, J. Nguyen, D.A. Kirschner, *J. Neurochem.* 62 (1994) 1203–1213.
- [7] J.M. Boggs, G. Rangaraj, *Biochemistry* 39 (2000) 7799–7806.
- [8] F.G. Mastronardi, C.A. Ackerley, A.I. Arsenault, B.I. Roots, M.A. Moscarello, *J. Neurosci. Res.* 36 (1993) 315–324.
- [9] A.E. Palma, P. Ow, C. Fredric, C. Readhead, M.A. Moscarello, *J. Neurochem.* 69 (1997) 1753–1762.
- [10] D.D. Wood, M.A. Moscarello, *J. Biol. Chem.* 264 (1989) 5121–5127.
- [11] R. Zand, X. Jin, D. Lubman, *Biochemistry* 37 (1998) 2441–2449.
- [12] F.C.-H. Chou, C.-H. Chou, R. Shapira, R.F. Kibler, *J. Biol. Chem.* 251 (1976) 2671–2676.
- [13] S. Cheifetz, M.A. Moscarello, *Biochemistry* 24 (1985) 1909–1914.
- [14] R. Martin, J.N. Whitaker, L. Rhame, R.R. Goodin, H.F. McFarland, *Neurology* 44 (1994) 123–129.
- [15] J.M. Boggs, G. Rangaraj, K.M. Koshy, C. Ackerley, D.D. Wood, M.A. Moscarello, *J. Neurosci. Res.* 57 (1999) 529–535.
- [16] J.M. Boggs, P.M. Yip, G. Rangaraj, E. Jo, *Biochemistry* 36 (1997) 5065–5071.
- [17] J.J. Ramsden, in: M. Malmsten (Ed.), *Biopolymers at Interfaces*, Dekker, New York, 1998, pp. 321–361, Chapter 10.
- [18] J.J. Ramsden, *Quart. Rev. Biophys.* 27 (1994) 41–105.
- [19] J.J. Ramsden, *Philos. Mag. B* 79 (1999) 381–386.
- [20] K. Tiefenthaler, *Adv. Biosensors* 2 (1992) 261–289.
- [21] J.R. Scherer, *Proc. Natl. Acad. Sci. USA* 84 (1987) 7938–7942.
- [22] J.J. Ramsden, J. Dreier, *Biochemistry* 35 (1996) 3746–3753.
- [23] K. Tiefenthaler, W. Lukosz, *J. Opt. Soc. Am. B* 6 (1989) 209–220.

- [24] L. Guemouri, J. Ogier, J.J. Ramsden, *J. Chem. Phys.* 109 (1998) 3265–3268.
- [25] G. Csúcs, J.J. Ramsden, *J. Chem. Phys.* 109 (1998) 779–781.
- [26] P.O. Luthi, J.J. Ramsden, B. Chopard, *Phys. Rev. E* 55 (1997) 3111–3115.
- [27] P. Schaaf, J. Talbot, *J. Chem. Phys.* 91 (1989) 4401–4409.
- [28] G. Tarjus, P. Viot, H.S. Choi, J. Talbot, *Phys. Rev. E* 49 (1994) 3239–3244.
- [29] E.L. Hinrichsen, J. Feder, T. Jøssang, *J. Stat. Phys.* 44 (1986) 793–827.
- [30] J.J. Ramsden, *Phys. Rev. Lett.* 71 (1993) 295–298.
- [31] P.R. Van Tassel, L. Guemouri, J.J. Ramsden, G. Tarjus, P. Viot, J. Talbot, *J. Colloid Interface Sci.* 207 (1998) 317–323.
- [32] D.R. Beniac, M.D. Luckevich, G.J. Czarnota, T.A. Tompkins, R.A. Ridsdale, F.P. Ottensmeyer, M.A. Moscarello, G.I. Harauz, Reconstruction via angular reconstitution of randomly oriented single particles, *J. Biol. Chem.* 272 (1997) 4261–4268.
- [33] R.A. Ridsdale, D.R. Beniac, T.A. Tompkins, M.A. Moscarello, G. Harauz, Considerations of predicted structures in multiple sclerosis, *J. Biol. Chem.* 272 (1997) 4269–4275.
- [34] J.J. Ramsden, G.I. Bachmanova, A.I. Archakov, *Phys. Rev. E* 50 (1994) 5072–5076.
- [35] J.J. Ramsden, *Colloids Surfaces B* 14 (1999) 77–81.
- [36] A. Gow, R. Smith, *Biochem. J.* 257 (1989) 535–540.
- [37] R. Kurrat, J.J. Ramsden, J.E. Prenosil, *J. Chem. Soc., Faraday Trans. 90* (1994) 587–590.
- [38] S. Cheifetz, M.A. Moscarello, C.M. Deber, *Arch. Biochem. Biophys.* 233 (1984) 151–160.
- [39] L.B. Pritzker, S. Joshi, J.J. Gowan, G. Harauz, M.A. Moscarello, *Biochemistry* 39 (2000) 5374–5381.
- [40] H. Wu, Y. Zheng, Z.-X. Wang, *Biochemistry* 42 (2003) 1129–1139.
- [41] L.B. Pritzker, S. Joshi, G. Harauz, M.A. Moscarello, *Biochemistry* 39 (2000) 5382–5388.
- [42] M. Yon, C.A. Ackerley, F.G. Mastronardi, N. Groome, M.A. Moscarello, *J. Neuroimmunol.* 65 (1996) 55–59.
- [43] C.M. Atkins, S.J. Chen, E. Klann, J.D. Sweatt, *J. Neurochem.* 68 (1997) 1960–1967.
- [44] J.K. Kim, F.G. Mastronardi, D.D. Wood, D.M. Lubman, R. Zand, M.A. Moscarello, *Mol. Cell. Proteomics* 2 (2003) 453–462.
- [45] C.M. Atkins, M. Yon, N.P. Groome, J.D. Sweatt, *J. Neurochem.* 73 (1999) 1090–1097.
- [46] F.G. Mastronardi, B. Mak, C.A. Ackerley, B.I. Roots, M.A. Moscarello, *J. Clin. Invest.* 97 (1996) 349–358.
- [47] C. Seiwa, I. Sugiyama, T. Yagi, T. Iguchi, H. Asou, *Neurosci. Res.* 37 (2000) 21–31.